第 44 卷 第 2 期/2024 年 1 月/光学学报 研究论文

光学学报

遗传算法宽光谱光学系统设计方法研究

陈阳*，王益清，高明，冯斌

西安工业大学光电工程学院光电信息技术研究所，陕西 西安 710021

摘要 针对宽光谱光学系统初始结构构建效率低、设计周期长的问题，提出基于遗传算法的宽光谱光学系统设计方法。推导等焦距、等像面成像条件，建立合理的优化目标函数，以光学结构参数作为遗传变量，利用研究的遗传算法解算出大量优异初始结构，筛选最优结构输入到光学仿真软件中，经过简单优化即可得到满足要求的宽光谱光学系统。以此方法设计了可见光、近红外宽光谱光学系统，系统成像波段为0.4～1.2 μm，焦距为40 mm，视场角均为±5°，波段范围内焦距差异小于0.03 mm，且宽光谱范围内成像质量良好。

关键词 宽谱段；遗传算法；等焦距；光学设计方法

中图分类号 TN214 **文献标志码** A **DOI**：10.3788/AOS231528

1 引 言

随着隐身、干扰技术的发展，窄光谱、单波段的成像光学系统已经无法满足复杂多变的应用环境[1-3]。在此背景下，宽光谱光学系统应运而生。宽光谱成像能够获取更全面、更精准的目标信息，有利于提升光电装备的探测及识别能力[4]。近年来，宽光谱、多波段光学系统得到了快速发展。此类系统在复杂使用环境中有着不可替代的重要作用。2013年Vizgaitis等[5]研制了集成式中波红外、长波红外宽光谱双视场成像系统，系统包含离轴反射式成像光组以及透射式中/长波波段成像光组。2020年Ju等[6]设计了一款视场范围为72°～110°的变焦距反射式系统，系统接收光谱包含可见光、长波红外两个波段。反射镜1和3分别充当变焦系统的变倍组及补偿组，两者同时移动保持像面稳定。同年，胡洋等[7]设计了一款红外宽光谱折衍混合光学系统。通过一组镜头，实现3.7～4.8 μm和7.7～10 μm双波段成像。2022年，王振东等[8]基于衍射光学理论，设计了一款工作波段为0.40～2.50 μm的宽波段成像系统，实现了可见光、近红外和短波红外波段的共孔径共焦面集成。

宽光谱光学系统性能优越，但其设计往往较为困难，究其原因主要是目前的光学设计方法并不完全适用于宽光谱系统设计，特别是宽光谱光学系统初始结构构建效率低，导致设计周期漫长[9-10]。为此，需要发展新型、高效的光学设计方法从而推动光学系统设计的进步[11-12]。本文对宽光谱光学系统设计方法进行探索，从理论层面分析系统齐焦、共像面条件，提出通过遗传算法解算焦距差异最优解，快速生成大量优秀初始结构的设计方法，在提升宽光谱共焦距光学系统设计效率的同时，为后期基于人工智能的光学系统设计提供训练样本。

2 初始结构设计方法

2.1 等焦距条件

为实现可见光到近红外宽光谱范围目标信息同步接收，要求成像光学系统在不同波长的焦距保持一致[13-14]，同时成像位置相同，即不同波长共焦距、共像面。然而，由于同种材料在不同波段的折射率是不相等的，根据单透镜的光焦度公式可知，经相同的透镜，各波段的焦距将存在差异。对于同一被测目标，光学系统的焦距不同会导致像的位置及大小产生差异。随着光谱范围的拓宽，成像差异不断增大。最终导致宽谱段范围内，图像为不同大小及位置光谱图像的混乱叠加，严重降低了系统成像质量。

$$\Phi=\begin{vmatrix} n-1 & n-1 \\ \dfrac{1}{r_1} & \dfrac{1}{r_2} \end{vmatrix}-\begin{vmatrix} \dfrac{(n-1)^2}{n} & 0 \\ 0 & \dfrac{d}{r_1 r_2} \end{vmatrix}, \tag{1}$$

式中：Φ为透镜光焦度；n为折射率；r_1、r_2为别透镜两个面的曲率；d为透镜厚度。

为了解决上述问题，本文提出了基于光焦度匹配

收稿日期：2023-09-05；**修回日期**：2023-10-09；**录用日期**：2023-10-21；**网络首发日期**：2023-11-01

基金项目：国家自然科学基金(62201454)、陕西省重点研发计划项目(2020GY-158)、2022年度“慧眼行动”成果转化应用项目(628020320)

通信作者：*867549558@qq.com

的多波段等焦距方法。虽然不同波段经过单透镜必然存在焦距差异，但当系统包含多组透镜时，不同透镜产生的焦距差异有可能相互抵消，通过合理地分配各光组光焦度能够使系统在各波段的焦距相等。

采用薄透镜理论，以两个波段、两个光组的系统为例说明等光焦度条件，双光组组合系统如图1所示。

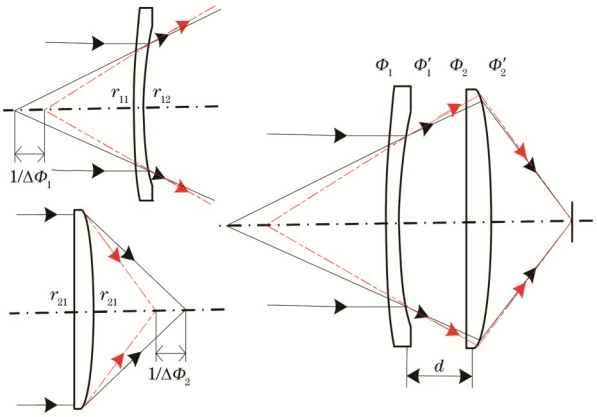

图1　等光焦度原理

Fig. 1　Equal focus principle

根据几何光学可推导出，双波段光学系统等光焦度的条件表示为

$$\Phi_{\lambda1}-\Phi_{\lambda2}=0\Rightarrow\begin{vmatrix}\Delta\Phi_1 & \Delta\Phi_2\\ -1 & 1\end{vmatrix}-d\begin{vmatrix}\Phi_1 & \Phi_2-\Delta\Phi_2\\ -\Delta\Phi_1 & \Delta\Phi_2\end{vmatrix}=0,\tag{2}$$

式中：$\Phi_{\lambda1}$、$\Phi_{\lambda2}$分别为两个波段的总光焦度；Φ_1、Φ_2分别为透镜1、2对应第一个波长的光焦度；$\Delta\Phi_1$、$\Delta\Phi_2$分别为两个透镜1、2在两个波段的光焦度差值。

根据几何光学知识，透镜的光焦度差异与透镜结构参数之间的关系满足

$$\Delta\Phi_i=\begin{vmatrix}\Phi_i & 0\\ 0 & \Phi_i'\end{vmatrix}=\begin{vmatrix}\Delta n_i & \Delta n_i\\ \dfrac{1}{r_{2i}} & \dfrac{1}{r_{2i-1}}\end{vmatrix}-\begin{vmatrix}\dfrac{\Delta n_i}{n_i(n_i+\Delta n_i)} & 0\\ 0 & \dfrac{d_i}{r_{2i-1}r_{2i}}\end{vmatrix},(i=1,2),\tag{3}$$

式中：Φ_i、Φ_i'分别为透镜i在两个波段的光焦度；r_{2i}、r_{2i-1}分别为透镜两个面的半径；d_i为透镜的中心厚度；n_i为某波长处透镜的折射率；Δn_i为两个波长透过该材料时折射率的差值。

对于包含k个光组的多波段光学系统，不同波段通过光学系统时的总光焦度为

$$\Phi_{\lambda1}=\sum_{i=1}^{k}\begin{vmatrix}\dfrac{h_i}{h_1} & 0\\ 0 & \Phi_i\end{vmatrix},\ \Phi_{\lambda2}=\sum_{i=1}^{k}\begin{vmatrix}\dfrac{h_i'}{h_1'} & 0\\ 0 & \Phi_i\end{vmatrix},\tag{4}$$

式中：h_i为光线在第i个透镜上的入射高度，在光学系统中近似认为$h_i=h_i'$。则不同波段间的光焦度差值为

$$\Delta\Phi=\Phi_{\lambda1}-\Phi_{\lambda2}=\sum_{i=1}^{k}\begin{vmatrix}\dfrac{h_i}{h_1} & 0\\ 0 & \Delta\Phi_i\end{vmatrix}。\tag{5}$$

将式(3)代入式(5)可得多光组系统等焦距条件为

$$\Delta\Phi=\sum_{i=1}^{k}\begin{vmatrix}\dfrac{h_i}{h_1} & 0\\ 0 & \Delta\Phi_i\end{vmatrix}=\sum_{i=1,2}\begin{vmatrix}\dfrac{h_i\Delta n_i}{h_1} & \Delta n_i\\ \dfrac{1}{r_{2i}} & \dfrac{1}{r_{2i-1}}\end{vmatrix}-\begin{vmatrix}\dfrac{h_i\Delta n_i}{h_1n_i(n_i+\Delta n_i)} & 0\\ 0 & \dfrac{d_i}{r_{2i-1}r_{2i}}\end{vmatrix}=0。\tag{6}$$

2.2　共像面条件

在宽光谱范围内，不同波长等焦距后，其成像位置仍可能存在差异。为了满足不同波长共像面成像，要求不同波长最终会聚位置到光学系统的距离相等，其可以用后截距l_F'表征。由几何光学知识可知，组合光学系统后截距可表示为

$$l_F'=\begin{vmatrix}f' & f'\\ \dfrac{d}{f_1'} & 1\end{vmatrix}=\begin{vmatrix}f' & f'\\ \dfrac{d(n-1)}{nr_1} & 1\end{vmatrix}。\tag{7}$$

对于包含k个折射面的光学系统，其组合系统后截距可表示为

$$l_F'=\begin{vmatrix}h_K & 0\\ 1 & \dfrac{1}{u_K'}\end{vmatrix}。\tag{8}$$

其中，h_k、u_k'可由几何光学公式递推得到

$$\begin{cases}n_2u_2=n_1'u_1'=n_1u_1+h_1\Phi_1,h_2=h_1-d_1u_1'\\ n_3u_3=n_2'u_2'=n_2u_2+h_2\Phi_2,h_3=h_2-d_2u_2'\\ \vdots\\ n_ku_k=n_k'u_k'=n_2u_2+h_k\Phi_k,h_k=h_{k-1}-d_{k-1}u_{k-1}'\end{cases}。\tag{9}$$

2.3　遗传算法共焦距、共像面初始结构设计方法

借鉴遗传算法[15-17]的思想，以各组元焦距和间隔作为个体参数，使用均匀创建函数随机生成若干光组作为个体，在设定的焦距、间隔及材料种群范围内，利用焦距差异目标函数选择出适应度高的优异粒子，结合后截距作为判定条件。对材料参数进行交叉迭代运算，对焦距及间隔进行变异迭代运算，使种群中其余个体向优异个体靠拢。经过多次运算求解出最优解及对应的各光组参数。若最优解达到适应度要求，则以此结果作为宽光谱系统的初始结构参数。若最优解未达到适应度函数要求，则继续搜索直到达到迭代次数

上限。

基于遗传算法的宽光谱光学系统初始结构的构建步骤如下。

1)设定参数。焦距搜索范围[$f'_{\min}$, $f'_{\max}$],间隔取值范围[$d_{\min}$, $d_{\max}$],材料种类范围[1, m],透镜数量 n,种群数量 P_n,波长参数[$\lambda_1, \lambda_2, \cdots, \lambda_n$]。

2)设定适应度函数。以不同波段的焦距差异作为适应度评价函数

$$\begin{cases} \mathrm{Target}(\Delta f'_{\lambda 1}) \\ \mathrm{Target}(\Delta f'_{\lambda 2}) \\ \vdots \\ \mathrm{Target}(\Delta f'_{\lambda n}) \end{cases}。 \tag{10}$$

3)生成初始种群。均匀随机生成个体,每个个体包含设定数量的光组以及光组的焦距、间隔和材料等参数

$$\begin{cases} \mathrm{Individual}_1[(f'_{1\lambda}, f'_{2\lambda}, \cdots, f'_{n\lambda})(d_{12}, d_{23}, \cdots, d_{nn-1})(G_1, G_2, \cdots, G_n)] \\ \mathrm{Individual}_2[(f'_{1\lambda}, f'_{2\lambda}, \cdots, f'_{n\lambda})(d_{12}, d_{23}, \cdots, d_{nn-1})(G_1, G_2, \cdots, G_n)] \\ \vdots \\ \mathrm{Individual}_n[(f'_{1\lambda}, f'_{2\lambda}, \cdots, f'_{n\lambda})(d_{12}, d_{23}, \cdots, d_{nn-1})(G_1, G_2, \cdots, G_n)] \end{cases}。 \tag{11}$$

4)计算适应度值。求解个体不同波段总焦距差异 $\Delta f'_{\lambda i}$

$$\begin{cases} \Delta f'_{\lambda 1} = \Delta F[\mathrm{Individual}_1(f'_{1\lambda}, f'_{2\lambda}, \cdots, f'_{n\lambda})(d_{12}, d_{23}, \cdots, d_{nn-1})(G_1, G_2, \cdots, G_n)] \\ \Delta f'_{\lambda 2} = \Delta F[\mathrm{Individual}_2(f'_{1\lambda}, f'_{2\lambda}, \cdots, f'_{n\lambda})(d_{12}, d_{23}, \cdots, d_{nn-1})(G_1, G_2, \cdots, G_n)] \\ \vdots \\ \Delta f'_{\lambda n} = \Delta F[\mathrm{Individual}_n(f'_{1\lambda}, f'_{2\lambda}, \cdots, f'_{n\lambda})(d_{12}, d_{23}, \cdots, d_{nn-1})(G_1, G_2, \cdots, G_n)] \end{cases}。 \tag{12}$$

5)选择最优个体。将焦距差异 $\Delta f'_{\lambda i}$ 作为适应度函数值,选择适应度值小的个体作为优异个体

$$(\Delta f'_{\lambda i})_{\min} = \mathrm{Optimal}(f'_i, d_i, G_i)。 \tag{13}$$

6)遗传运算。设定材料交叉运算,个体变异运算,对焦距、间隔以及材料进行遗传迭代,从而求解最优解

$$\begin{cases} \mathrm{Crossover}(A, B) = \mathrm{Crossover\ operation}\left[(G_{A1}, G_{A2}, \cdots, G_{An}) \times \dfrac{1}{\Delta f'_A}, (G_{B1}, G_{B2}, \cdots, G_{Bn}) \times \dfrac{1}{\Delta f'_B}\right]。 \\ \mathrm{Mutation}(A_{i+1}) = \mathrm{Mutation\ operation}[A_i + (I_{\mathrm{Optimal}} - A_i)a_i + (I_{\mathrm{Optimal}} - A_i)b_i + c_i] \end{cases} \tag{14}$$

7)焦距差异检测。将计算得到的不同波段焦距差异与设定条件进行对比,检测解算结果是否满足共焦要求,

$$\sum \Delta f'_{\lambda i} = \mathrm{Constraint}(\Delta f'_{\lambda i})。 \tag{15}$$

若满足要求,则输出初始结构参数

$$\begin{aligned} &\mathrm{Initial\ optical\ system} = \\ &(f'_{1\lambda n\mathrm{th}}, f'_{2\lambda n\mathrm{th}}, \cdots, f'_{i\lambda n\mathrm{th}}, \cdots, f'_{n\lambda n\mathrm{th}}), \\ &(d_{1n\mathrm{th}}, d_{2n\mathrm{th}}, \cdots, d_{in\mathrm{th}}, \cdots, d_{nn\mathrm{th}})。 \end{aligned} \tag{16}$$

8)若不满足要求,重复步骤 5~7,直至满足焦距差异目标函数或者达到迭代次数上限。

9)从焦距差异目标函数的个体中筛选满足像面差异要求的个体作为初始结构。

3 系统指标及初始结构解算

拟设计的光学系统包含可见光、近红外波段,要求设计的系统各波段焦距一致,视场角相等,系统各波段性能指标如表 1 所示。

利用研究的遗传算法构建最优初始结构,根据设计指标在软件中设定初始结构的中心波长、焦距 f_i' 取值范围、d 间距取值范围、材料库、光组数量、种群数量、随机步长系数、总焦距及焦距差异目标函数等,具体设置参数如表 2 所示。系统波长为 0.4~1.2 μm,其跨越可见光到近红外波段,为保证生成初始结构焦距差异在整个波段范围内一致,分别取 0.55 μm、1.1 μm 作为典型中心波长。

表 1 初始结构系统指标

Table 1 Initial structural system indicator

Parametric	Target
Wave band /μm	0.4-1.2
Focal length /mm	40
Focal length difference /mm	<0.5
Optimal image plane difference /mm	<0.5
Field of view /(°)	±5
F number	3.5

在设定参数初值后,软件按顺序生成材料组合,设定的材料数为 4,透镜数量为 5,则理论上存在 1024 种材料组合。每种组合按平均分布随机生成 100 组种群。设定运行时间 1 h,对每一组随机种群进行约 20 次遗传算法迭代。得到初始结构的焦距差异结果如图 3 所示。在 1024 种组合中,有 407 组达到焦距差异要求,其为宽光谱光学系统设计提供大量满足目标函数的初始结构,有利于缩短此类系统设计周期。

初始结构选择首先考虑不同波段焦距差异、像面

表 2 具体设置参数表

Table 2 Specific setting parameter

Parametric	Target
Center wave length /μm	0.55 and 1.1
Focal length range /mm	[10,100]
Interval range /mm	[1,50]
Combination of materials	[1,4]
Number of lenses	5
Number of population	100
Focal length /mm	40
Focal length difference /mm	<0.5

位置差异，从 407 组优秀结构中选取焦距差异最小的 5 组，对比分析其光焦度分布，并要求透镜径厚比不大于 1∶10，透镜边缘厚度不小于 5 mm，尝试进行优化，发现第 127 组优化结果最好。最终选择第 127 组作为初始结构，参数如表 3 所示。其在可见光 0.55 μm 波段的焦距为 39.98 mm，近红外 1.1 μm 波段的焦距为 40.02 mm，可见光波段像面位置 17.31 mm，近红外波段像面位置 17.42 mm。将构建的初始结构参数输入到光学设计模拟软件，得到其光路图如图 4 所示。

4 设计结果及性能评价

4.1 设计结果

将解算的可见光、近红外宽光谱初始结构输入到光学设计软件，经简单优化后得到最终系统结构如图 5 所示，其可以同步接收可见光到近红外波段信息。不同波长焦距均为 40 mm，像面位置相同，且具有系统透镜数量少、体积小、质量轻的特点。

4.2 像质分析

图 6 为宽光谱范围内的调制传递函数(MTF)图，可以看出，0.4～1.2 μm 波段在奈奎斯特频率 100 lp/mm 处，轴上点高于 0.55，轴外点高于 0.5。图 7 为 0.4～1.2 μm 波段的点列图，可以看出，弥散斑最大均方根值为 2.472 μm，总体来看系统成像质量良好。

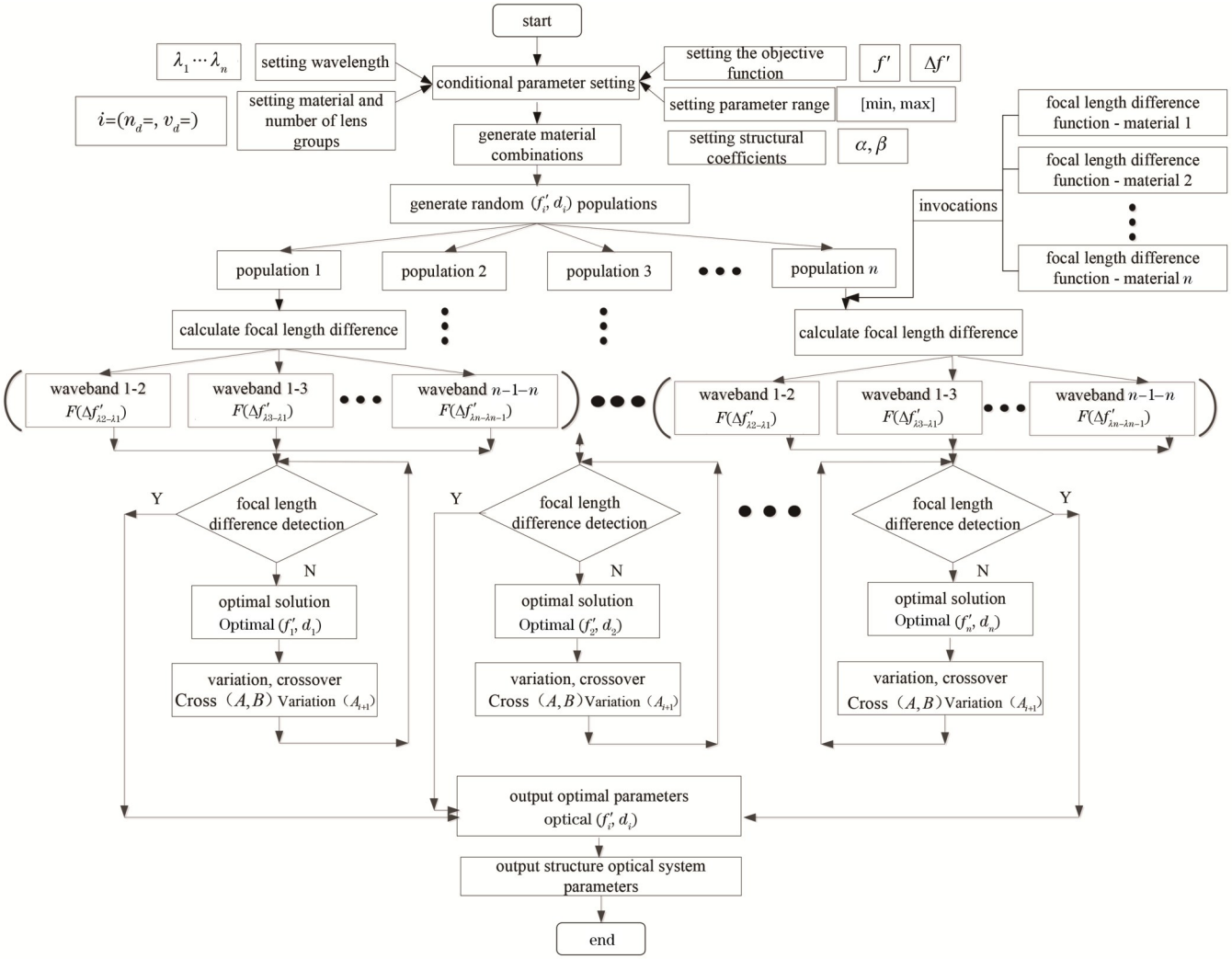

图 2 初始结构构建流程图

Fig. 2 Construction process diagram of initial structure

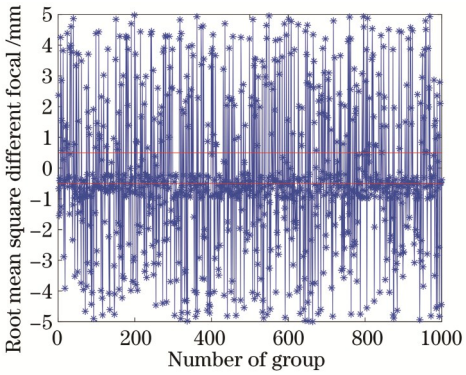

图 3　遗传算法迭代结果图

Fig. 3　Iteration result graph of genetic algorithm

表 3　第 127 组初始结构参数

Table 3　Initial structural parameters of the 127th group

Surface	Radius /mm	Thickness /mm	Glass
OBJ	Infinity	Infinity	
1	22.342	3.000	H-FK61
2	Infinity	1.000	
3	19.652	2.900	H-FK61B
4	Infinity	2.000	
5	−20.014	2.000	H-ZLAF50E
6	20.014	3.687	
7	18.911	3.000	H-ZPK5
8	−18.911	1.000	
STO	Infinity	7.592	
10	−107.950	2.000	H-ZLAF50E
11	55.680	17.311	
IMA	Infinity		

Notes: OBJ is object surface, STO is stop surface, IMA is image surface.

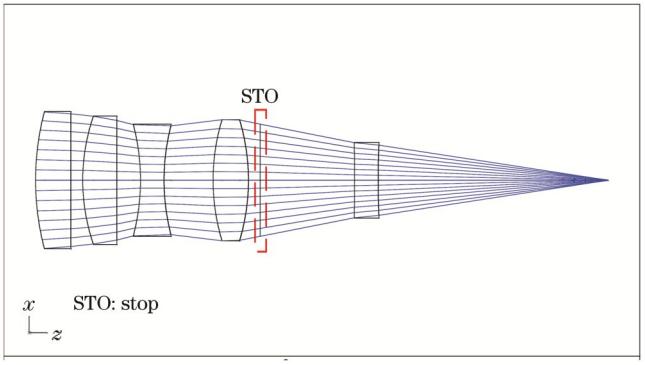

图 4　初始结构图

Fig. 4　Schematic diagram of the initial structure

5　系统共焦距、共像面分析

图 8 给出了宽光谱光学系统色焦移曲线，该曲线反映了系统焦距随波长的变化情况。可以看出，波段范围内焦移为 −0.010～0.018 mm，小于 0.03 mm。图 9 给出了宽光谱光学系统传递函数随视场变化曲线，可以看出，整个视场范围内光线会聚基本都在最佳成像位置，说明宽光谱范围内光线会聚良好。

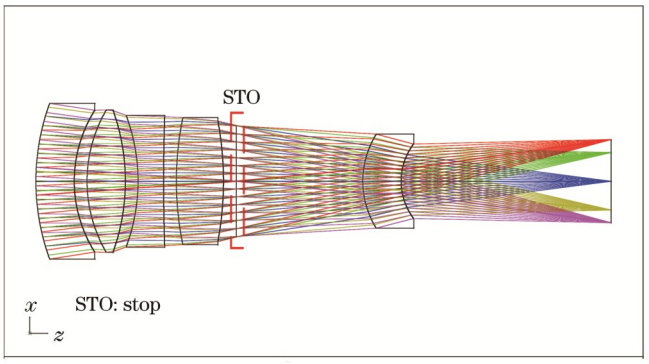

图 5　系统结构图

Fig. 5　System architecture diagram

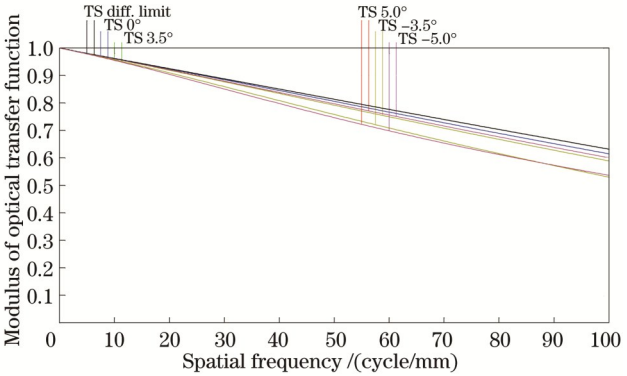

图 6　0.4～1.2 μm 波段 MTF 图

Fig. 6　MTF map of 0.4—1.2 μm band

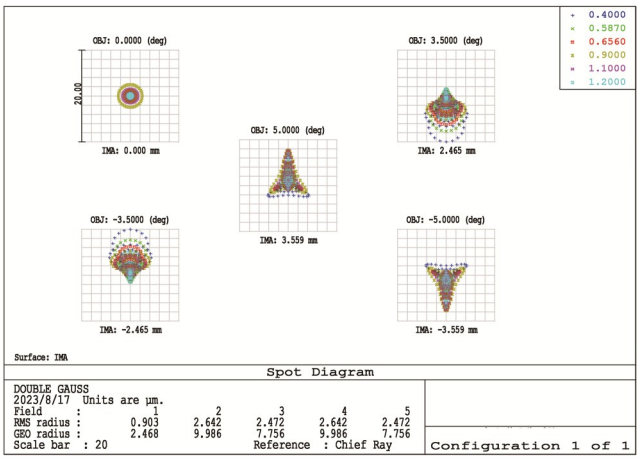

图 7　0.4～1.2 μm 波段点列图

Fig. 7　Spot diagram of 0.4-1.2 μm band

6　结　　论

为了提升宽光谱类光学系统的设计效率，本文研究了基于遗传算法的宽光谱光学系统设计理论及方法。推导宽光谱共焦距、共像面方程，确定焦距差异及

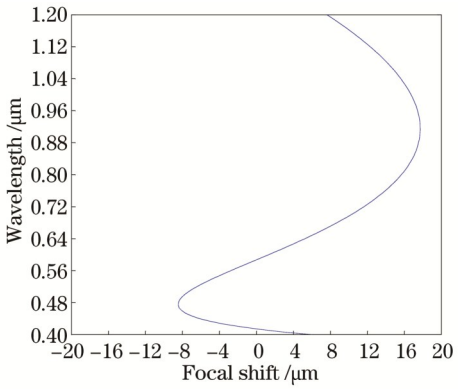

图 8 焦移随波长变化曲线

Fig. 8 Curve of focal shift changing with wavelength

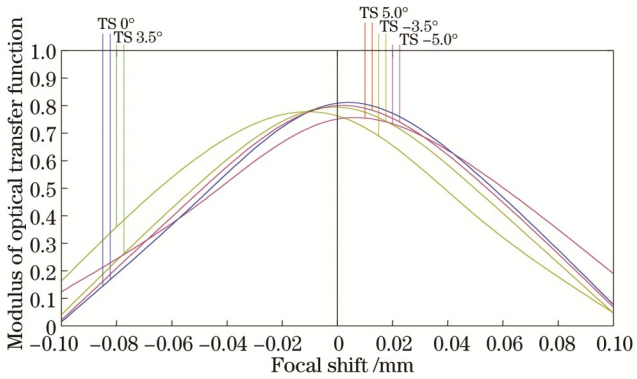

图 9 MTF 随视场变化

Fig. 9 MTF changes with field of view

像面差异适应度函数，建立遗传算法光学结构参数变异、材料交叉初始结构生成算法。为验证算法的可行性及效率，设计了一款可见光、近红外宽光谱光学系统。设计结果表明，在遗传算法宽光谱光学系统构建方法一次性生成种群中，有 407 个迭代个体达到了目标函数要求。该算法通过短时间迭代得到大量潜在的相对最优解，提升了宽光谱光学系统的设计效率，同时大量优秀初始结构为后期基于人工智能的光学系统设计提供训练样本。在未来的工作中将开展优秀结构判别条件及筛选算法的研究，确定自动评判因素及权重，进一步通过对比最终优化结果及时效，对初始结构生成及优选算法进行改进和评价。

参 考 文 献

[1] Ming G, Yang C, Jun L, et al. Design of dual-band shared-aperture co-zoom optical system[J]. Infrared Physics & Technology, 2014, 64: 40-46.

[2] Hartke J P, Dereniak E L. Snapshot dual-band visible hyperspectral imaging spectrometer[J]. Optical Engineering, 2007, 46(1): 013201.

[3] Yahyanejad S, Rinner B. A fast and mobile system for registration of low-altitude visual and thermal aerial images using multiple small-scale UAVs[J]. ISPRS Journal of Photogrammetry and Remote Sensing, 2015, 104: 189-202.

[4] 宣斌, 赵泽宇, 罗曜伟, 等. 宽光谱可见-短波红外成像光学系统设计[J]. 红外与激光工程, 2023, 52(4): 20220638.
Xuan B, Zhao Z Y, Luo Y W, et al. Design of optical system for wide-spectrum visible-short wave infrared imaging[J]. Infrared and Laser Engineering, 2023, 52(4): 20220638.

[5] Vizgaitis J N, Hastings A R, Jr. Dual band infrared picture-in-picture systems[J]. Optical Engineering, 2013, 52(6): 061306.

[6] Ju Y J, Jo J H, Ryu J M. Optical design of reflecting omnidirectional zoom optical system with peripheral half-field of view from 110° to 72° for day and night surveillance[J]. Optik, 2020, 212: 164690.

[7] 胡洋, 崔庆丰, 孙林, 等. 红外双波段折衍混合光学-数字联合系统设计[J]. 光学学报, 2020, 40(14): 1422002.
Hu Y, Cui Q F, Sun L, et al. Optical-digital joint design of a dual-waveband infrared refractive-diffractive system[J]. Acta Optica Sinica, 2020, 40(14): 1422002.

[8] 王振东, 刘欢, 陈阳, 等. 基于谐衍射理论的 0.40 ~ 2.50 μm 宽波段光学系统设计[J]. 激光与光电子学进展, 2022, 59(19): 1922002.
Wang Z D, Liu H, Chen Y, et al. Design of 0.40-2.50 μm wide-band optical system based on harmonic diffraction theory[J]. Laser & Optoelectronics Progress, 2022, 59(19): 1922002.

[9] 吴羽婷, 林志强, 王敏. 15 mm ~ 300 mm 宽光谱变焦光学系统设计[J]. 应用光学, 2023, 44(3): 491-499.
Wu Y T, Lin Z Q, Wang M. Design of 15 mm-300 mm wide-spectrum zoom optical system[J]. Journal of Applied Optics, 2023, 44(3): 491-499.

[10] 常宇梅, 王劲松. 轻小型宽波段变焦物镜光学系统设计[J]. 光学学报, 2023, 43(8): 0822029.
Chang Y M, Wang J S. Design of lightweight and miniaturized zoom objective optical system with wide band[J]. Acta Optica Sinica, 2023, 43(8): 0822029.

[11] 陈兴涛, 苏宙平, 张杨柳, 等. 基于正交种子曲线扩展算法设计自由曲面离轴反射无焦系统[J]. 光学学报, 2022, 42(1): 0108001.
Chen X T, Su Z P, Zhang Y L, et al. Design of freeform off-axis reflective afocal systems by orthogonal seed curve extension algorithm[J]. Acta Optica Sinica, 2022, 42(1): 0108001.

[12] 杨通, 段璎哲, 程德文, 等. 自由曲面成像光学系统设计：理论、发展与应用[J]. 光学学报, 2021, 41(1): 0108001.
Yang T, Duan Y Z, Cheng D W, et al. Freeform imaging optical system design: theories, development, and applications [J]. Acta Optica Sinica, 2021, 41(1): 0108001.

[13] 陈阳, 高明, 胡雪蕾, 等. 共口径宽光谱复眼光学系统设计[J]. 光子学报, 2020, 49(3): 0322002.
Chen Y, Gao M, Hu X L, et al. Design of co-aperture wide spectrum compound eye optical system[J]. Acta Photonica Sinica, 2020, 49(3): 0322002.

[14] 党更明, 高明, 范晨, 等. 红外双波段共焦复合孔径光学系统设计[J]. 光学学报, 2023, 43(8): 0822019.
Dang G M, Gao M, Fan C, et al. Design of infrared dual-band confocal composite aperture optical system[J]. Acta Optica Sinica, 2023, 43(8): 0822019.

[15] 徐奉刚, 黄玮. 遗传算法在离轴四反光学系统设计中的应用[J]. 光学 精密工程, 2017, 25(8): 2076-2082.
Xu F G, Huang W. Application of genetic algorithm in the design of off-axis four-mirror optical system[J]. Optics and Precision Engineering, 2017, 25(8): 2076-2082.

[16] Yu Z Z, Yang Z, Zhang Y, et al. Optimized design for illusion device by genetic algorithm[J]. Scientific Reports, 2021, 11: 19475.

[17] Wu X F, Zhou E Z, Tu L J, et al. Optimal determination of resistance coefficient of heating pipe network based on genetic algorithm[J]. Engineering Research Express, 2021, 3(4): 045001.

Design Method of Broad-Spectrum Optical System by Genetic Algorithm

Chen Yang*, Wang Yiqing, Gao Ming, Feng Bin

Institute of Optical Information Technology, School of Optoelectronic Engineering, Xi'an Technological University, Xi'an 710021, *Shaanxi, China*

Abstract

Objective Broad-spectrum optical systems have superior performance. They can obtain more comprehensive and accurate target information and are conducive to enhancing the detection and identification capabilities of optoelectronic equipment. In addition, they have an irreplaceable role in complex environments. However, their design is often difficult, and the current main optical design method is to optimize the selected initial structure, but the initial structure of the broad-spectrum optical system is inefficiently constructed. Therefore, the design cycle is long, and it relies too much on the experience of the designers. In this paper, we explore the design method of broad-spectrum optical systems, analyze the system's confocal and co-image plane conditions from the theoretical level, and focus on the initial structure construction method of broad-spectrum systems based on a genetic algorithm.

Methods Firstly, a multi-band equal focus method based on optical focus matching is proposed to derive the equal optical focus condition by taking a system with two bands and two optical groups as an example, and the system's focal lengths in each band are set to be equal by reasonably allocating the optical focus of each optical group. Then, in order to meet the different wavelengths of the common image plane imaging, the geometric optics formula recursively obtains the combined system of equal image plane conditions. The idea of a genetic algorithm is used to independently construct the optical group composition and structure form of the broad-spectrum optical system and iteratively solve the optimal initial structure, and the selection of the optimal group is based on the experience of the designers, which is mainly considered in the differences in the focal lengths of different wavelengths, the differences in the position of the imaging surface, the distribution of the optical focal lengths, the ratio of the lens diameter to thickness, and the thickness of the edge of the lens, and other aspects. Finally, the selected optimal initial structure is optimized to obtain a broad-spectrum optical system with a small number of lenses, small volume, light weight, and good imaging quality.

Results and Discussions For the same target, different focal lengths will lead to differences in the position and size of the image, and with the broadening of the spectral range, the imaging differences increase, which will seriously reduce the imaging quality of the system. The theoretical derivation of this paper obtains the conditions of equal focal lengths and co-image surfaces, which can solve this problem. For the optimal initial structure construction of the transmissive system, this paper independently constructs the optical group composition and structural form of the system by genetic algorithm, while the existing papers use optimization algorithms for the design of reflective systems, such as the design of reflective free-form surfaces. In the initial structure construction process of such systems, the parameters of the incident light and the requirements of the outgoing light are determined, and the algorithm process actually fits the reflective surface according to the laws of geometrical optics under the premise of known incident and outgoing light. In contrast, the transmissive system contains multiple optical groups; the light propagation path inside the system is completely uncertain, and the number of optical groups and the structure form are all unknown. Therefore, the main framework strategy and process of the broad-spectrum initial structure construction algorithm in this paper are completely different. In addition, we generate many possible optimal solution results through the powerful computational ability of the algorithm, which ensures a high probability of occurrence of the optimal solution by the number and effectively prevents the algorithm from falling into the local optimum. The results of the algorithm (Fig. 3) indicate that it can efficiently generate a large number of excellent initial structures of the broad-spectrum system, providing training samples for the later AI-based optical system design.

Conclusions In this paper, we derive the broad-spectrum co-focal distance and co-image plane equations, determine the focal distance difference and image plane difference fitness function, and establish the genetic algorithm structure parameter variation and material crossover method. In order to verify the feasibility and efficiency of the method, a visible and near-infrared broad-spectrum optical system is designed, and the system has an imaging band of 0.4 - 1.2 μm and a focal length of 40 mm. The difference in the focal length within the range of the band is less than 0.03 mm, and the imaging quality is good in the broad-spectrum range. The design results show that the genetic algorithm-based broad-spectrum optical system construction method can generate 1024 excellent populations at a time, of which 407 iterative individuals can meet the requirements of the objective function. The appropriate optimal solution is input into the Zemax software for optimization, and a broad-spectrum optical system that meets the requirements can be obtained very quickly. In summary, the proposed genetic algorithm can shorten the design cycle and improve the design efficiency of broad-spectrum optical systems.

Key words broad spectrum; genetic algorithm; equal focal length; optical design method